Process simulation development of a clean waste-to-energy conversion power plant Thermodynamic and environmental assessment

Kuo, Po Chih; Illathukandy, Biju; Kung, Chi Hsiu; Chang, Jo Shu; Wu, Wei

DOI
10.1016/j.jclepro.2021.128156

Publication date
2021

Document Version
Final published version

Published in
Journal of Cleaner Production

Journal of Cleaner Production 315 (2021) 128156

Contents lists available at ScienceDirect

Journal of Cleaner Production

journal homepage: www.elsevier.com/locate/jclepro

Process simulation development of a clean waste-to-energy conversion power plant: Thermodynamic and environmental assessment

Po-Chih Kuo [a,*], Biju Illathukandy [b,c], Chi-Hsiu Kung [d], Jo-Shu Chang [e,f,g], Wei Wu [e]

[a] Process and Energy Department, Faculty of 3mE, Delft University of Technology, Leeghwaterstraat 39, 2628, CB, Delft, the Netherlands
[b] Centre for Rural Development & Technology, Indian Institute of Technology, Delhi, India
[c] Department of Mechanical Engineering, Government Engineering College, Kozhikode, Kerala, India
[d] Occupational Safety and Health Department, Tayih Corporation, Tainan, 702, Taiwan
[e] Department of Chemical Engineering, National Cheng Kung University, Tainan, 70101, Taiwan
[f] Department of Chemical and Materials Engineering, Tunghai University, Taichung, 407, Taiwan
[g] Research Center for Smart Sustainable Circular Economy, Tunghai University, Taichung, 407, Taiwan

ARTICLE INFO

Handling editor: Kathleen Aviso

Keywords:
Waste to energy conversion
Energy and environmental analysis
Gasification
CO_2 capture
Process integration
EROI

ABSTRACT

Waste-to-energy (WTE) conversion technologies for generating renewable energy and solving the environmental problems have an important role in the development of sustainable circular economy. This paper presents a novel high-efficiency WTE power plant using refuse-derived fuel (RDF) as feedstock by integrating torrefaction (T) pretreatment with plasma gasifier (PG), solid oxide fuel cell (SOFC), and combined heat and power (CHP) system. The combined impacts of torrefaction conditions (i.e. temperature and residence time) and steam-to-fuel (S/F) ratio on the energy and environmental performances of the proposed T-PG-SOFC-CHP power plant without CO_2 capture (System I) is first evaluated. Results show that torrefaction of RDF prior to plasma gasification provides better syngas quality and therefore the system electrical efficiency (SEE) and CHP efficiency (CHPE) of System I can be markedly boosted compared to that of untreated RDF. However, the integration of torrefaction unit shows a negative effect on the energy return on investment (EROI) due to high energy demands for torrefaction and plasma gasification. Overall, the values of CHPE of System I range from 47.25% to 55.39% when the torrefaction temperatures of 200 and 250 °C are adopted. In contrast, the torrefaction of RDF at 300 °C is not a recommended condition for operation in the T-PG-SOFC-CHP power plant because of noticeably negative energy and environmental impacts. Moreover, to prevent the risk of carbon deposition on the SOFC anode, a recirculation ratio (RR) of the anode off-gas of 30% is required. Finally, the introduction of oxy-fuel combustion technology into the T-PG-SOFC-CHP system for CO_2 capture (System II) allows to achieve a zero direct CO_2 emission WTE power plant. However, this results in an energy penalty of about 5.40–6.77% associated with the CO_2 capture and compression process.

1. Introduction

With the significantly increasing growth of global population, economy, and urbanization, the amount of waste produced by different industrial sectors are also increasing at a quick rate. According to the "World Bank Group's" report, global annual waste production is estimated to increase from 2.01 billion tons in 2016 to 3.40 billion tons by 2050, accounting for a rise of around 70% (Kaza et al., 2018). In particular, this will also lead to substantial amount of CO_2 emissions to the environment if the waste is ultimately landfilled without energy recovery (Manfredi et al., 2009). To improve waste management and sustainability, in the recent years, efficient waste-to-energy (WTE) conversion technologies have received considerable attention worldwide (Putna et al., 2020). The WTE conversion technologies render a great potential for promoting environmental savings as a result of CO_2 emissions prevented through energy recovery (Boesch et al., 2014).

In general, thermo-chemical conversion technologies such as incineration, pyrolysis, gasification, and hydrothermal carbonation are promising to convert solid waste into heat and electricity (Al-asadi et al., 2020). Among them, waste gasification provides a sustainable, economical, and environment friendly solution (Ng et al., 2019). The desired quality of syngas (H_2+CO), depending on the type of gasifying

* Corresponding author.
E-mail addresses: pckuo225@gmail.com, p.c.kuo@tudelft.nl (P.-C. Kuo).

https://doi.org/10.1016/j.jclepro.2021.128156
Received 6 March 2021; Received in revised form 26 June 2021; Accepted 28 June 2021
Available online 29 June 2021

agents such as air, steam or steam-air mix, can be generated from this process. On the other hand, compared with the conventional gasification, the utilization of plasma technology in waste gasification has currently attracted increasing attention since it offers several advantages: (1) owing to the high operating temperature and heating rate, various kinds of hazardous waste can be effectively converted into useful form of energy (Rutberg et al., 2013); (2) a high-quality syngas, mainly consisting of hydrogen and carbon monoxide can be produced, thereby improving the lower heating value (LHV) of the product gas (Saleem et al., 2020); and (3) negligible tar level in the product gas as the decomposition of tar is nearly completed under a high temperature environment (Ma et al., 2020).

The benefits revealed above from the plasma gasification (PG) technology gave a great opportunity to develop a high-efficiency WTE process via integrating PG with solid oxide fuel cells (SOFCs). Typically, the operating temperature of SOFC is between 700 and 1000 °C, which closely approaches the gasification temperature, meaning that it is possible to produce a thermal integration of the PG and SOFC systems (Liu et al., 2014). Besides, by virtue of the high temperature operation of SOFCs, the exhaust heat can be easily coupled with a gas-turbine (GT) cycle or a combined heat and power (CHP) system for producing additional electricity. It has been reported that such hybrid systems can not only generate clean electricity at high efficiencies (~50–70%), but also have a high potential for stable, durable, and reliable long-term operations (Recalde et al., 2018). Therefore, in contrast to the conventional coal-fired or IGCC power plant, an integrated gasification-SOFC system provides more environment friendly and energy efficient system.

To explore the technical feasibility and applications of an integrated PG-SOFC system for the WTE conversion process, Liu et al. (2014) preliminarily evaluated the combined PG-SOFC-CHP system using faecal matter as a feedstock. The net electrical and heat efficiencies of such a system without drying unit were calculated as 11.68% and 44.99%, respectively, accounting for a CHP efficiency of 56.67%. Perna et al. (2018) proposed an integrated air plasma gasification fuel cell (IAPGFC) to convert municipal solid waste (MSW) into heat and electricity. They reported that varying the oxygen content from 40% to 100% in the plasma gas, the electrical efficiency of the proposed IAPGFC system increased from 34.6 to 40.1%, which was higher than that of a conventional integrated waste gasification combined cycle plant (33%), whereas the reference IAPGFC plant using air (21% oxygen) had an electrical efficiency of 29% only. Recalde et al. (2018) developed a PG-SOFC power plant to treat faecal sludge for sanitation applications. Their simulated results pointed out that with waste heat recovery design, the net electrical and exergy efficiencies of such a system can reach up to 65.3% and 57.8% respectively.

Recently, considerable attention has also been paid to the torrefaction of waste for the applications of WTE technologies, which is helpful for upgrading the inherent drawbacks of the raw solid waste. For instance, Rago et al. (2020) torrefied three types of MSWs (Mango branches, waste newspaper, and low-density polyethylene) at 300 °C for 30 min and indicated that the fixed carbon and carbon contents, and calorific values of the torrefied MSWs increased, while the volatile matter, oxygen and hydrogen contents decreased after experiencing torrefaction. Additionally, due to the improved properties of the torrefied MSWs, the combustion performance of co-firing of coal with the torrefied MSWs could also be boosted. Iroba et al. (2017) investigated the characteristics of torrefied construction demolition waste (CDW) through microwave-assisted technology and concluded that with appropriate process conditions, torrefaction can significantly reduce the energy consumption for grinding of CDW and improve the pellet density and hydrophobicity. Edo et al. (2017) concluded that torrefaction technology plays an important role in the reduction of environmental impact during WTE process. Two types of fuel blends (MSW and RDF) with demolition and construction (DC) wood were used to study the effect of torrefaction on the ash-forming elements contained in the char and toxic emissions of pollutants (polychlorinated dibenzo-p-dioxins (PCDD) and dibenzofurans (PCDF)). They found that torrefaction can significantly reduce the chlorine content in the char and lowers the emission of PCDD and PCDF during the combustion of torrefied char. Hence, according to the recent studies regarding the utilization of torrefaction in waste treatment, it is clearly revealed that torrefaction is a prospective and potential approach to make the solid waste more uniform, efficient, and viable for downstream applications such as combustion and gasification (Recari et al., 2017).

Based on the research papers reviewed above, it is apparent that both the PG-SOFC power generation systems and the torrefaction pretreatment are attractive and efficient methods to be applied in the WTE conversion route. However, an examination of the literature shows that there are no studies that assessed the impact of torrefaction of solid waste on the plasma gasification performance, nor any works on the integration of torrefaction (T) with the PG-SOFC based power plant. Accordingly, the major aim of this work is to assess a new integrated T-PG-SOFC-CHP power plant's performance in terms of energy efficiency and environmental impact analysis. To achieve the above objectives, a conceptual process design and thermodynamic simulation model of the T-PG-SOFC-CHP power plant is first developed in Aspen Plus. The combined effects of torrefaction process conditions of RDF (i.e. temperature and residence time) and steam-to-fuel ratio (S/F ratio) on the performance of the plasma gasification and the overall T-PG-SOFC-CHP system (System I) is then investigated in detail. Next, a sensitivity analysis of fuel utilization factor (U_f), and recirculation ratio (RR) of the anode-off gas is performed to find the optimum operating conditions. On the other hand, an oxy-fuel combustion technology for CO_2 capture has a great potential to couple with the SOFC systems to achieve a zero-carbon emission power generation system (Thattai et al., 2017). Consequently, the second aim of this study is to design a new oxy-fuel combustion-based T-PG-SOFC-CHP power plant for achieving zero direct CO_2 emissions (System II) and then to compare its energy and environmental performances with System I. The energy penalty associated with the oxy-fuel combustion CO_2 capture and storge for System II is also discussed.

2. Process modeling and description

A novel WTE power plant consisting of four main subsystems including T, PG, SOFCs, and CHP is developed using Aspen Plus V10. In the simulation, the Peng-Robinson Boston Mathias equation of state is chosen as the thermodynamic property (Kuo and Wu, 2016a). Two configurations of the T-PG-SOFC-CHP power plant with and without CO_2 capture are simulated and compared using refuse-derived fuel (RDF) as feedstock. The overall process concept to produce heat and clean electricity from RDF is presented in Fig. 1, where the proposed integrated system is made of six units consisting of a torrefaction, a plasma gasification, a gas cleaning unit, SOFCs, an oxy-fuel combustion for CO_2 capture (for System II), and a CHP system. The detailed process model of each subsystem is described below, while the process

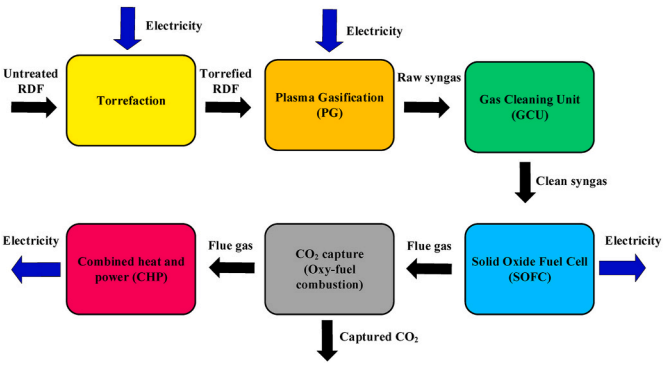

Fig. 1. Process concept of a novel waste-to-energy conversion power plant.

descriptions of CHP cycle is given elsewhere (Kuo and Wu, 2016b). To achieve a better understanding, the overall framework of the T-PG-SOFC-CHP system modeling analysis is depicted in Fig. 2. On the other hand, the detailed operating conditions of each main subsystem are summarized in Table 1.

2.1. Plasma gasification model

The schematic of the proposed T-PG-SOFC-CHP power plant without CO_2 capture is illustrated in Fig. 3 (System I). To make a comparison, a base case using the untreated RDF (without torrefaction) as a feedstock is first studied. According to Nobre et al. (2019), the raw RDF was obtained from a waste company (CITRI, S.A., Setúbal, Portugal) and was processed in a mechanical treatment plant to reduce its particle size (average size: 30 mm). Alternatively, various torrefied RDFs (TRs) are produced under different torrefaction conditions at various torrefaction temperatures (200 °C, 250 °C, and 300 °C) and residence times (15 min, 30 min, and 60 min). Accordingly, ten scenarios named as untreated RDF, TR200-15, TR200-30, TR200-60, TR250-15, TR250-30, TR250-60, TR300-15, TR300-30, and TR300-60 are compared in terms of energy and environmental performances. The physical and chemical properties of the raw RDF and different TRs are acquired from the experimental work, in which a series of RDF torrefaction experiments were performed, and they are listed in Table 2 (Nobre et al., 2019). In addition, the model is established according to the following key assumptions in the development of the T-PG-SOFC-CHP power plant: (1) a steady-state modelling is developed; (2) the feedstock is fed at ambient conditions; (3) the solid and gaseous phases are in a state of thermodynamic equilibrium; and (4) the graphitic carbon is used to represent char in the simulation (Kuo et al., 2014). Based on the proximate and elemental analysis of RDF (Table 2), the fuels and ash are defined as non-conventional components in Aspen Plus. Moreover, the HCOALGEN model is chosen to estimate the heat of combustion, heat of formation, and heat capacity of fuels, while the DCOALIGT model is selected to calculate the density of biomass fuels (Kuo et al., 2014).

For the base case, the flowrate of the feedstock stream (S1) is fixed at 50 kg h^{-1} of untreated RDF and it is fed to a plasma gasifier, as shown in Fig. 3. In contrast, for the T-PG-SOFC-CHP power plant integrated with torrefaction pretreatment, the untreated RDF is first torrefied in a torrefaction reactor (B1). As shown in Table 3, the torrefaction characteristics of RDF such as mass yield, energy yield, and energy demand are obtained from the same experimental study and thus different experimental data sets are taken into account to simulate the torrefaction behavior (Nobre et al., 2019). After undergoing torrefaction, TR is then

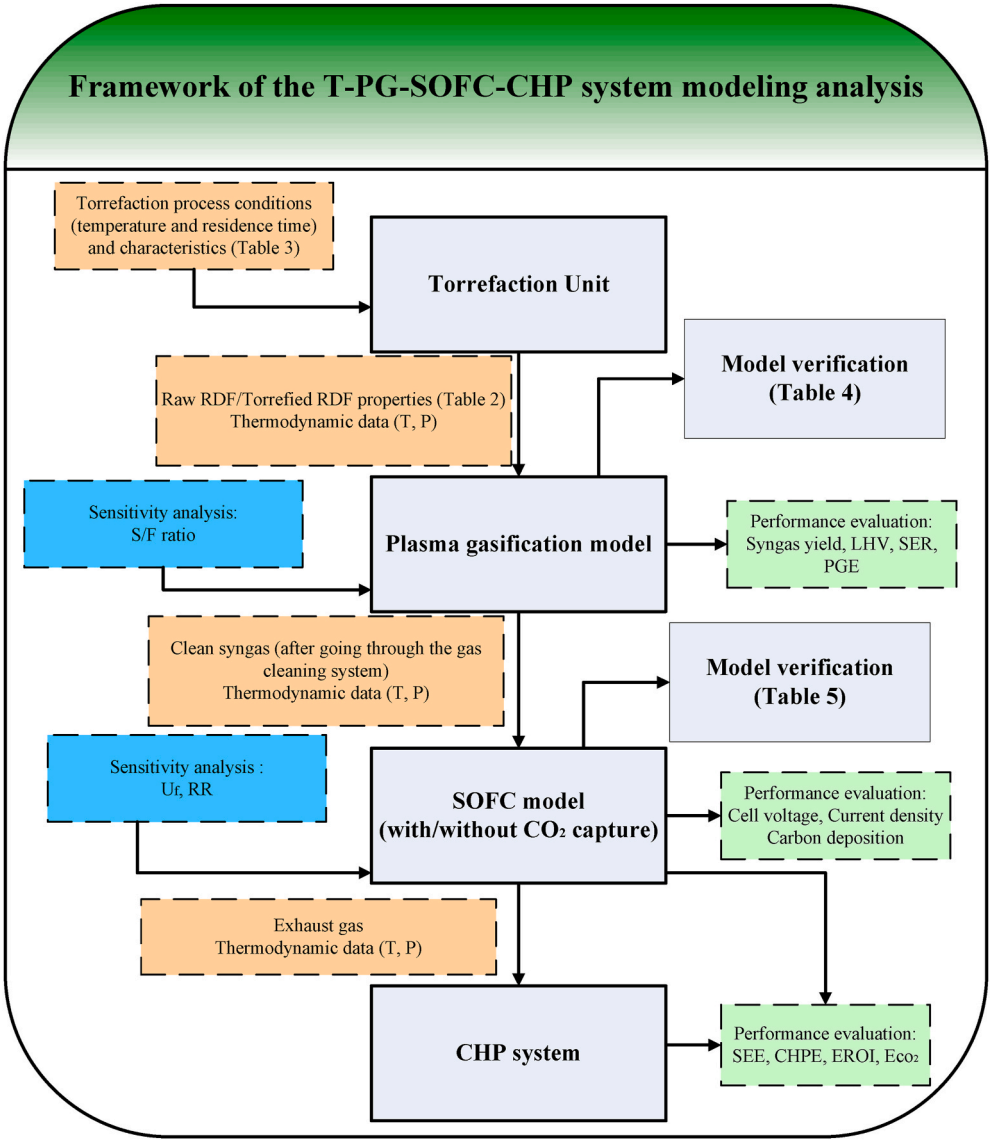

Fig. 2. Flowchart of the T-PG-SOFC-CHP system modeling analysis.

Table 1
Simulation parameters used in the proposed T-PG-SOFC-CHP power plant.

Units	Parameters	Value	Reference
Torrefaction	Inlet fuel flow rate (kg hr^{-1})	10–100	-
	Temperature (°C)	200–300	Nobre et al. (2019)
	Residence time (min)	15, 30, 60	Nobre et al. (2019)
Plasma gasifier	S/F ratio (−)	0.01–0.6	–
	Gasifier temperature (°C)	2500	Janajreh et al. (2013)
	Torch temperature (°C)	4000	Janajreh et al. (2013)
	Torch efficiency (%)	85	Mazzoni and Janajreh (2017)
Solid oxide fuel cell	Temperature (°C)	900	Thattai et al. (2017)
	Pressure (atm)	1	Zhang et al. (2005)
	Fuel utilization factor (−)	0.65–0.90	Zhang et al. (2005)
	Recirculation ratio of the anode off-gas (%)	0–40	Colpan et al. (2007)
	DC/AC conversion efficiency (%)	95	Thattai et al. (2017)
HRSG and steam turbine cycle	Inlet pressure of high/intermediate/low turbines (bar)	125/19/3.7	Xiang et al. (2020)
	Isentropic efficiency of high/intermediate/low pressure turbines (%)	92/84/90	Xiang et al. (2020)
	Mechanical efficiency of turbines (%)	98	Kuo and Wu (2016a)
Oxy-fuel combustion	Oxygen excess (%)	5	Sheng et al. (2014)
	Combustion temperature (°C)	1400	Xiang et al. (2018)
	Specific energy consumption for O_2 production (kWh kg^{-1})	0.269	Esfilar et al. (2018)
CO_2 compression	Temperature (°C)	35	Martínez et al. (2018)
	Pressure (bar)	150	Martínez et al. (2018)

sent to the plasma gasifier, which is established by a number of Aspen Plus blocks. An RYield (B2) is used to convert non-conventional fuel (S3) into conventional components (S4) (i.e. H_2, O_2, N_2, S, solid carbon, and ash) via a calculator block with external FORTRAN subroutines in accordance with the component characteristics of raw RDF (Table 2). A separator (B3) accounts for the simulation of the evaporation of the water content contained in the RDF. The outlet flow of the separator (S6) is subsequently sent to two gasification reactors including a high temperature (HT) and a low temperature (LT) reactor to model the various plasma gasification reactions. In this regard, two RGibbs reactors based on the chemical and phase equilibrium calculations by minimizing the Gibbs free energy are used (Janajreh et al., 2013). The HT reactor (B4) and LT reactor (B6) are operated at 2500 and 1250 °C, respectively (Minutillo et al., 2009). Furthermore, another separator (B5) is installed between HT reactor and LT reactor in order to remove the slag generated during the plasma gasification. The plasma gas (steam) is heated from 25 °C (S5) to 4000 °C (S7) by using a DC non-transferred plasma torch which is simulated by a heater (H3) in Aspen Plus (Janajreh et al., 2013). An electrical plasma efficiency of 85% is assumed in this study (Mazzoni and Janajreh, 2017).

Next, the produced hot raw syngas (S14) is passed through a gas cleaning unit to remove the main impurities such as sulfur compounds before sending it to the SOFC system. A ZnO-based desulfurization unit is utilized to remove H_2S, as follows:

$$ZnO + H_2S \leftrightarrow ZnS + H_2O, \quad \Delta H^0 = -78.89\ kJ\ mol^{-1} \tag{R1}$$

Based on the experimental work of Spies et al. (2017) for H_2S removal from simulated coal derived-syngas, the optimal operating temperature of the ZnO sorbent reactor for the adsorption of H_2S was found to be 450 °C. As a result, the raw syngas (S15) produced from the plasma gasifier is first cooled down to 450 °C though a cooler (C1) and then passed through the ZnO bed to remove H_2S, which is modeled using an Requil block (B8) in Aspen Plus.

2.2. Solid oxide fuel cell model

The SOFC model is also developed in the Aspen Plus environment and the detailed process descriptions and assumptions of the SOFC model are reported elsewhere in a previous study (Kuo and Wu, 2016a). In brief, an RGibss block based on Gibbs free energy minimization is utilized to model the chemical reactions occurring at the anode, while a separator is used to model oxygen required by the electrochemical reactions (Zhang et al., 2005). The clean syngas (S16) is pressurized to 3 atm ($P_{syngas}/P_{SOFC} = 3$) using a compressor (B9) (Doherty et al., 2010). A mixer (B10) is used to mix the recycled anode off-gas (S23) with fresh syngas (S18). The mixed gas (S20) is subsequently fed to the SOFC anode, while the pretreated air (S21) is sent to the SOFC cathode. To calculate the required amount of oxygen ($nO_{2,required}$) to react with hydrogen at the SOFC anode, a design specification block is used in the cathode unit by implementing the following equations in Aspen Plus.

$$U_f = \frac{nH_{2,consumed}}{nH_{2,equivalent}} = \frac{I \times 0.018665}{nH_{2,\text{equivalent}}} \tag{1}$$

$$nO_{2,required} = 0.5(U_f)(nH_{2,equivalent}) \tag{2}$$

$$U_a = \frac{nO_{2,consumed}}{nO_{2,in}} \tag{3}$$

where U_f is the fuel utilization factor, $nH_{2,\text{consumed}}$ is the molar flow rate of hydrogen reacted at the anode (kmol h^{-1}), $nH_{2,equivalent}$ is the equivalent hydrogen (kmol h^{-1}), I is the cell current (A), U_a is the air utilization factor, $nO_{2,consumed}$ is the molar flow rate of oxygen reacted at the cathode (kmol h^{-1}), and $nO_{2,in}$ is the molar flow rate of oxygen fed into the cathode (kmol h^{-1}).

With regard to the cell voltage and current density calculation, the detailed equations for the Nernst voltage and cell voltage loss caused by the ohmic, activation, and concentration polarizations are provided in the Appendix, while the geometry parameters and material properties used in this study are based on the study of Doherty et al. (2010). After the cell voltage (V_{cell}) is calculated, the SOFC power output is then calculated as follows:

$$W_{SOFC,AC} = W_{SOFC,DC} \times \eta_{inv} = I \times V_{cell} \times \eta_{inv} \tag{4}$$

where V_{cell} is the cell voltage (V), and η_{inv} is the inverter efficiency (%).

To avoid the carbon deposition at the SOFC anode, the anode off-gas of SOFC enters into a splitter block (B11), which is used to control the amount of the anode off-gas in the recycle loop. The recirculation ratio (RR) of anode off-gas is defined as:

$$Recirculation\ ratio\ (RR) = \frac{\dot{m}_{recycle}}{\dot{m}_{anode\ off-gas}} \times 100(\%) \tag{5}$$

where $\dot{m}_{recycle}$ and $\dot{m}_{anode\ off-gas}$ are the mass flow rates of the recycled anode gas (S23) and outlet anode off-gas (S22) (kg hr^{-1}) respectively.

The anode off-gas is then sent to a combustor (B12) where oxidation of the unreacted hydrogen and carbon monoxide take place to release heat. An RStoic block which is a stoichiometry-based reactor is utilized to model the combustion reaction. Next, the hot exhaust gas (S26) from the combustor flows through a heat exchanger (EX-1) in order to preheat the cathode air, and then sent to a CHP system, including a heat recovery steam generator (HRSG) and a three-stage steam turbine (ST) cycle to generate additional electricity.

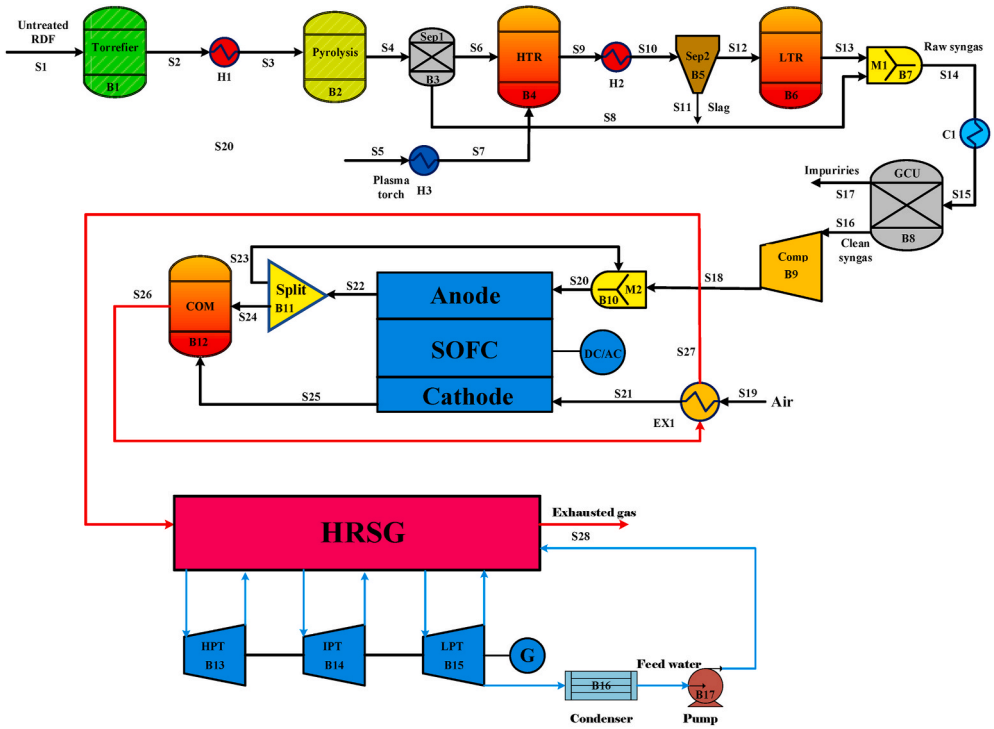

Fig. 3. Schematic of a T-PG-SOFC-CHP power plant without CO_2 capture (System I).

Table 2
Properties of the raw and torrefied RDF (TR) at various torrefaction process conditions used in the simulation (Nobre et al., 2019).

Torrefaction conditions (temperature-residence time)	Raw RDF	TR200-15	TR200-30	TR200-60	TR250-15	TR250-30	TR250-60	TR300-15	TR300-30	TR300-60
Proximate analysis (wt%, dry basis)										
Moisture	6.02	2.10	1.40	1.09	1.60	1.80	1.70	1.60	0.60	0.40
Volatile matter	82.6	82.5	82.5	82.2	80.7	79.4	75.8	77.0	68.3	62.4
Fixed carbon	9.2	9.2	8.3	10.0	11.0	12.0	11.6	14.0	22.3	25.8
Ash	8.2	8.3	9.3	7.8	8.3	8.6	12.70	9.0	9.4	11.8
Elemental analysis (wt%, dry-ash-free)										
C	36.7	43.4	48.0	47.5	41.1	47.8	53.3	53.5	56.7	59.5
H	4.1	6.1	6.7	6.4	5.5	5.9	6.0	6.0	5.4	5.1
N	1.3	0.7	0.4	0.7	0.9	1.3	0.7	1.0	0.9	1.0
O	57.4	49.5	44.7	45.1	52.2	44.6	39.7	39.3	36.7	34.1
S	0.6	0.3	0.3	0.3	0.4	0.3	0.3	0.2	0.3	0.3
LHV (MJ kg^{-1})	17.8	17.5	18.3	18.5	17.4	18.5	19.3	19.9	20.7	20.9

Table 3
Torrefaction characteristics at various process conditions used in the simulation (Nobre et al., 2019).

Torrefaction conditions (temperature-residence time)	Mass yield (%)	Energy yield (%)	Energy requirements for torrefaction (MJ)
TR200-15	96.8	94.6	1.81
TR200-30	95.9	97.6	1.77
TR200-60	94.5	97.7	1.63
TR250-15	96.3	93.6	1.82
TR250-30	94.4	98.3	1.85
TR250-60	90.0	96.9	1.77
TR300-15	80.6	90.0	2.49
TR300-30	75.0	86.7	2.68
TR300-60	72.4	84.7	2.65

2.3. SOFC based oxy-fuel combustion design for CO_2 capture

Fig. 4 displays the second schematic of T-PG-SOFC-CHP power plant with CO_2 capture (System II). In this design, an oxy-fuel combustion technology is introduced to the SOFC system. Similar to System I, the untreated RDF is first torrefied and gasified to produce clean syngas, which is then fed to the SOFC for power generation. However, in System II, the CO_2 capture subsystems including an air separation unit (ASU) (B13), an oxy-fuel combustor (B12), and CO_2 compression and sequestration units (B20) are added into the T-PG-SOFC-CHP power plant. The ASU is modeled by using a separator block where 99.99 mol % of oxygen (S28) is separated from the air. The specific energy consumption of 0.269 kWh kg^{-1} is considered for pure oxygen production in the ASU (Esfilar et al., 2018). The anode off-gas (S24) is combusted with pure oxygen with a 5% excess to produce high temperature flue gas (S27), mainly comprising of CO_2 and steam (Sheng et al., 2014). A part of the flue gas is recycled (S31) by using a splitter block (B14) in order to control the combustion temperature to 1400 °C (Xiang et al., 2018). After passing through the HRSG unit to recover heat and produce electricity, the water contained in the flue gas is further condensed in a condenser, thereby generating a CO_2-rich gas (S32). The high purity CO_2 gas is then compressed to a final pressure of 150 bar (S33) through a multi-stage compressor block (B20) for further sequestration and storage (Martínez et al., 2018).

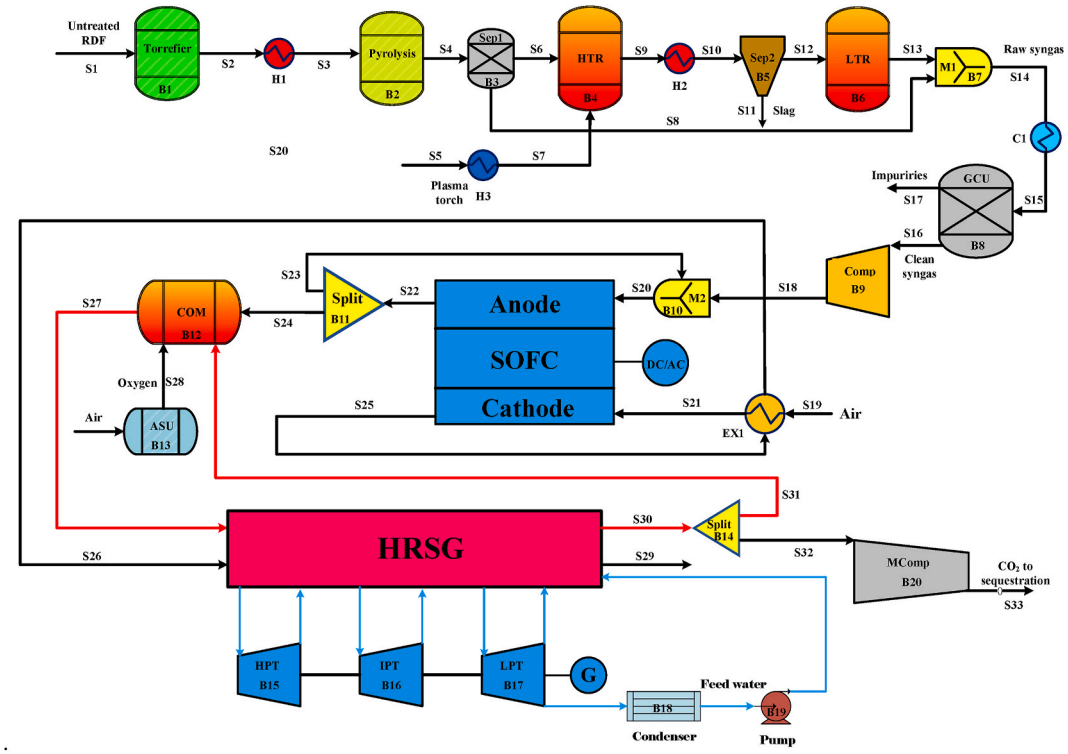

Fig. 4. Schematic of an oxy-fuel combustion-based T-PG-SOFC-CHP power plant with CO_2 capture (System II).

2.4. Model validation

To verify the accuracy of the developed plasma gasifier model, two studies of Minutillo et al. (2009) and Janajreh et al. (2013) from the literature are used for validation. Five various cases chosen to compare the present results and their feedstock and operating conditions are listed in Table 4. Fig. 5 shows a comparison of syngas composition and the plasma torch power between our simulated results and the literature. It can be seen that the results from our developed plasma gasifier and from the validated studies are all in good agreement. Hence, the developed plasma gasifier is suitable and reliable to predict the plasma gasification performance.

The SOFC model has been validated against the data reported by the studies of Zhang et al. (2005) and Doherty et al. (2010). In the study of Zhang et al. (2005), a model of the SOFC fueled by natural gas was developed in Aspen Plus and its cell voltage was calculated based on the semi-empirical correlations. The first comparison is reported elsewhere in a previous study, where the model validation showed a very good agreement between our predicted results and reported data (Kuo and Wu, 2016a). To further examine the reliability and suitablility of the proposed model, a second comparison of the SOFC model running on syngas is conducted by considering the cell geometry parameters for the cell voltage calculation. The molar fractions of H_2, CO, CO_2, CH_4, H_2O, and N_2 in the syngas were 34%, 16%, 15.8%, 7.4%, 25.7%, and 1.1%, respectively, which was produced by the Güssing DFB gasifier with an operating temperature of 850 °C and a steam/fuel ratio of 0.75 (Doherty et al., 2010). The operating temperature, pressure, and active area of the SOFC were 910 °C, 1.09 bar, and 96.1 m^2, respectively. The fuel utilization and air utilization factors were fixed at 0.85, and 0.167 respectively, and a targeted DC power of 120 kW was generated (Doherty et al., 2010). Table 5 summarizes the predictions of the developed SOFC model in comparison with the results obtained from Doherty et al. (2010). It is clear that the simulated results from our proposed model are also in line with the literature. Therefore, it is concluded that the proposed plasma gasifier and SOFC models are capable of predicting the performance of an integrated plasma gasifier-SOFC system in this study.

Table 4
Summary of operating conditions used for the validation of plasma gasifier (Minutillo et al., 2009; Janajreh et al., 2013).

Case	Feedstock	Gasifying agents	Plasma gas/fuel ratio	Outlet syngas temperature (°C)	Reference
A	RDF[a]	Air	0.782	1250	Minutillo et al. (2009)
B	RDF[a]	O_2 (vol. 40%) N_2 (vol. 60%)	0.643	1250	Minutillo et al. (2009)
C	RDF[a]	Air O_2	0.505 0.207	1250	Minutillo et al. (2009)
D	MSW[b]	Air Steam	0.36 0.56	1267	Janajreh et al. (2013)
E	Coal	Air Steam	1.31 0.7	1264	Janajreh et al. (2013)

[a] RDF: refused-derived fuel.
[b] MSW: municipal solid waste.

2.5. System parameters and performance indicators

A steam-to-fuel (S/F) ratio, as shown in Eq. (6), is used to investigate the performance of plasma gasifier.

$$S/F = \frac{\dot{m}_{steam}}{\dot{m}_{RDF}} \tag{6}$$

where $\dot{m}_{steam}$ and $\dot{m}_{RDF}$ are the mass flow rate of plasma gas (steam) and the untreated RDF, respectively (kg hr^{-1}).

To evaluate the plasma gasification performance, two indicators, plasma gasification efficiency (PGE) (%) and specific energy requirement (SER) (kWh kg^{-1}), are calculated by using Eq. (7)-Eq. (10).

$$PGE\ (\%) = \frac{\dot{m}_{product\ gas} LHV_{product\ gas}}{\dot{m}_{RDF} LHV_{RDF} + W_{torrefaction} + W_{plasma}} \times 100\% \tag{7}$$

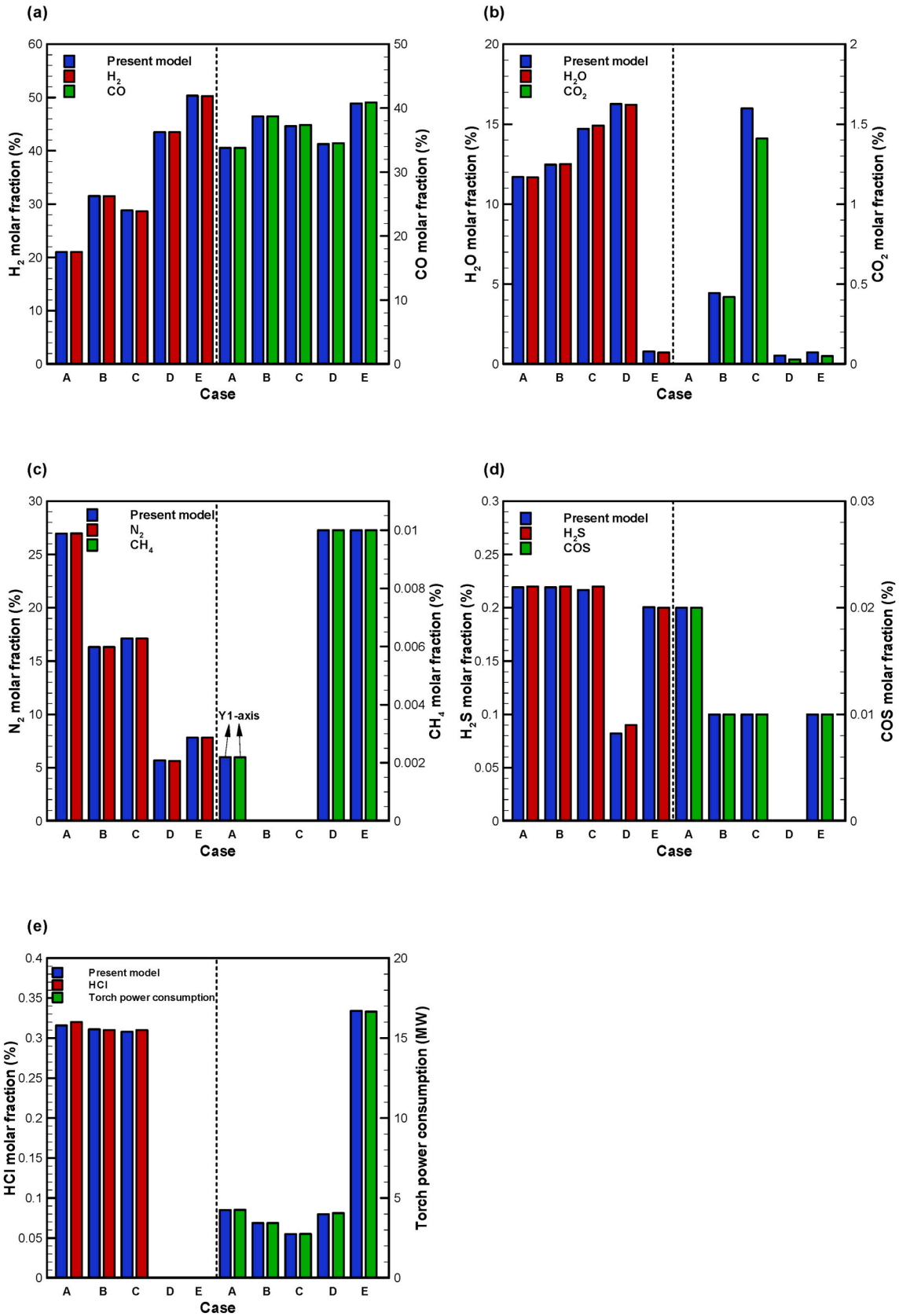

Fig. 5. Validation of the plasma gasifier model: (a) H_2 and CO, (b)H_2O and CO_2, (c)N_2 and CH_4, (d) H_2S and COS, and (e) HCl and torch power consumption.

Table 5
Comparison of the validation results of SOFC model with the data obtained from literature (Doherty et al., 2010).

Gas composition (mol%)	Pre-reformer outlet stream		Anode outlet stream		Cathode outlet stream	
	Present model	Reference	Present model	Reference	Present model	Reference
H_2	29.42	29.4	6.26	6.2	0	0
CO	7.20	7.2	4.15	4.2	0	0
CO_2	25.82	25.8	30.0	30.0	0	0
CH_4	3.54	3.6	0	0	0	0
H_2O	32.99	33.1	58.64	58.7	0	0
N_2	1.03	1.0	0.95	0.9	81.86	81.9
O_2	0	0	0	0	18.14	18.1
SOFC performance	Voltage (mV)		Current density (mA/m^2)		Gross AC efficiency (LHV)	
	Present model	Reference	Present model	Reference	Present model	Reference
	663.7	662	188.2	188.7	42.65	42.53

$$W_{plasma} = \frac{W_{torch}}{\eta_{torch}} \tag{8}$$

$$LHV_{product\ gas} = x_{H_2} LHV_{H_2} + x_{CO} LHV_{CO} + x_{CH_4} LHV_{CH_4} \tag{9}$$

$$SER = \frac{W_{plasma}}{\dot{m}_{syngas}} \tag{10}$$

where $\dot{m}_{product\ gas}$ is the mass flow rate of product gas from the plasma gasifier (kg hr^{-1}). $W_{torrefaction}$, W_{plasma}, W_{torch} are the energy requirement of torrefaction process, plasma energy, and torch power (kW), respectively. η_{torch} is the plasma torch efficiency (%). $LHV_{product\ gas}$, LHV_{RDF}, LHV_{H_2}, LHV_{CO}, and LHV_{CH_4} are the lower heating value of the product gas, the untreated RDF, H_2, CO, and CH_4, respectively (MJ kg^{-1}). x_{H_2}, x_{CO}, x_{CH_4} are the mass fractions of H_2, CO, CH_4 in the product gas, respectively. $\dot{m}_{syngas}$ is the mass flow rate of syngas (H_2 and CO) (kg hr^{-1}).

The system electrical efficiency (SEE) and combined heat and power efficiency (CHPE) are calculated to evaluate the overall performance of the T-PG-SOFC-CHP system. They are defined as follows:

$$SEE\ (\%) = \frac{W_{net}}{\dot{m}_{RDF} LHV_{RDF}} \times 100\% \tag{11}$$

$$W_{net} = W_{gross} - \sum W_{aux} \tag{12}$$

$$CHPE\ (\%) = \frac{W_{net} + Q}{\dot{m}_{RDF} LHV_{RDF}} \times 100\% \tag{13}$$

where W_{net} is the net power output of the overall system (kW) and W_{gross} is the gross power output of SOFC and steam turbines (kW). $\sum W_{aux}$ denotes the sum of auxiliary power (kW) which includes energy consumption related to torrefaction, plasma gasification, air separation unit, gas compressors, and water pumps. Q stands for the useful thermal energy from the T-PG-SOFC-CHP power plant (kW).

In addition to the energy efficiency analysis two environmental performance indicators are also addressed, namely, energy return on investment (EROI) and specific CO_2 emissions (E_{CO_2}) of the WTE power plant. The EROI is defined as the ratio of useful energy delivered (output) to the life cycle primary energy demand (input) from the non-renewable source to produce that energy, as expressed in Eq. (14) (Zhang and Colosi, 2013). Hence, higher the EROI, the more the potential benefits to the society. The life-cycle system boundary of the proposed T-PG-SOFC-CHP power plant is shown in Fig. 1. It is to be noted that the energy required for fuel processing and transportation, and infrastructure construction is not considered in the EROI and the specific CO_2 emissions calculation.

$$EROI = \frac{Energy\ \ delivered\ \ (kW)}{Energy\ \ required\ \ (kW)} \tag{14}$$

The specific CO_2 emissions of the T-PG-SOFC-CHP power plant can be determined as per the following equation:

$$Net\ \ CO_2\ \ emissions\ (kg\ hr^{-1}) = CO_2\ \ direct\ \ emissions + CO_2\ \ indirect\ \ emissions \tag{15}$$

$$E_{CO_2}\ \ (kg\ kWh^{-1}) = \frac{Net\ \ CO_2\ \ emissions}{W_{net}} \tag{16}$$

where the direct CO_2 emissions represent the total CO_2 produced from the T-PG-SOFC-CHP power plant, while the indirect CO_2 emissions are caused by the auxiliary power consumption (from the non-renewable source).

In this work, a CO_2 emission factor of 0.655 kg CO_2 kWh^{-1} is adopted for calculating the indirect CO_2 emissions (Ramirez et al., 2019).

3. Results and discussion

In this section, the combined influences of torrefaction process conditions (i.e. temperature and residence time) and S/F ratio on the performance of an integrated T-PG system is first investigated to find the optimum operating conditions with respect to the S/F ratio. The untreated RDF (without torrefaction) is also studied to make a comparison. Subsequently, the energy and environmental performances of the overall T-PG-SOFC-CHP power plant without CO_2 capture (System I) is evaluated to understand the most appropriate torrefaction process conditions for the proposed WTE process. The results are further used to carry out a series of sensitivity analyses in terms of U_f and RR of anode off-gas. Finally, the oxy-fuel combustion-based T-PG-SOFC-CHP system with CO_2 capture (System II) is analyzed to compare the energy and environmental performances with System I.

3.1. Plasma gasification performance

Fig. 6 shows the effect of S/F ratio on the variations of the mole flow rate of H_2 (Fig. 6a), CO (Fig. 6b), CO_2 (Fig. 6c) and CH_4 (Fig. 6d) from the plasma gasification of RDF with respect to different torrefaction conditions. Overall, the amount of H_2 and CO_2 production increases with the increasing S/F ratio, whereas that of CO and CH_4 production displays a maximum distribution with an exception to the untreated RDF. It is well documented that both water gas reaction ($C + H_2O \rightarrow CO + H_2$) and water gas shift reaction ($CO + H_2O \leftrightarrow CO_2 + H_2$) mainly contribute to H_2 production during steam gasification (Kuo and Wu, 2016b). The trend of CO concentration with increasing S/F ratio is attributed to the following reactions. It is first produced due to the water gas reaction and then consumed to produce CO_2 due to the water gas shift reaction as shown in Fig. 6b and c. The trend of CH_4 formation exhibited a peak value and then declined similar to that of CO formation (Fig. 6d). The increasing trend of CH_4 is mainly attributed to methanation reaction ($C + 2\,H_2 \leftrightarrow CH_4$), but with a further rise in the S/F ratio, the steam

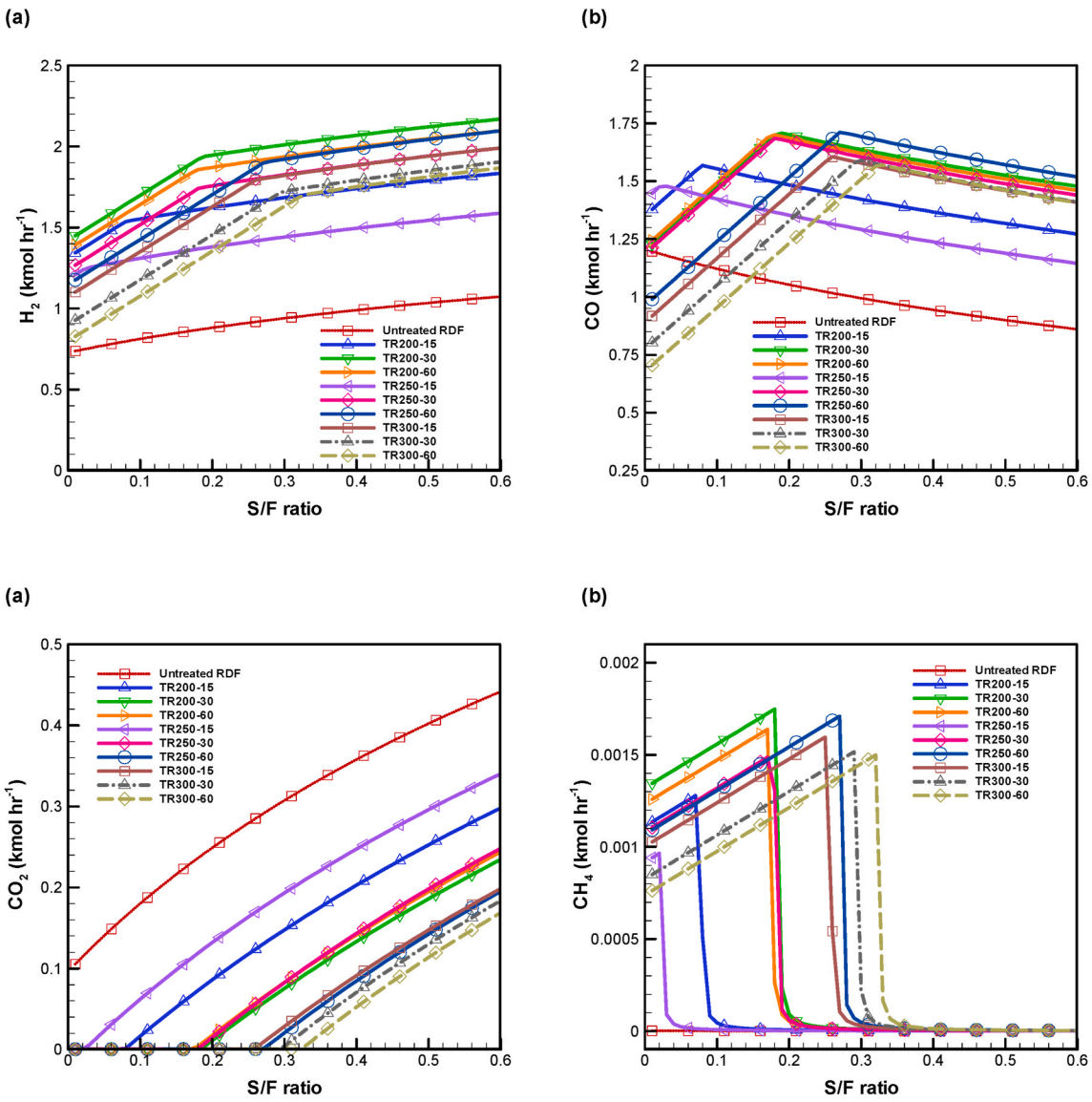

Fig. 6. Effect of S/F ratio on the product gas distribution from the plasma gasifier: (a) H_2, (b) CO, (c) CO_2, and (d) CH_4.

methane reforming reaction ($CH_4 + H_2O \leftrightarrow CO + 3H_2$) is favored. On the other hand, from a comparison of gas production from the plasma gasifier between the untreated and torrefied RDF, it can be seen that the former displayed the lowest amount of H_2 production and the highest amount of CO_2 production. Additionally, unlike the case of torrefied RDF, the trend of CO production decreases linearly with increasing S/F ratio. These observations can be ascribed to low carbon content and high oxygen content in the untreated RDF (Table 2).

Fig. 7a displays that the syngas yield of the untreated RDF can be improved significantly after torrefaction under suitable S/F ratios. The highest syngas yield is 1.03 kg kg-fuel^{-1} for the cases of TR200-30 and TR250-60, which is found at S/F = 0.19 and S/F = 0.27, respectively. Furthermore, it is worth noting that although the carbon content in the RDF obviously increases at a torrefaction temperature of 300 °C, the syngas yield of TR300-15, TR300-30, and TR300-60 are even lower than that of TR200-30 and TR250-60. This fact can be attributed to a significant mass loss of RDF materials in the course of torrefaction, which is up to 19.4% for TR300-15, 25% for TR300-30, and 27.6% for TR300-60 (Table 3). Fig. 7b shows the lower heating value (LHV) of the product gas (Eq. (9)). It can be observed that the values of LHV of the untreated and torrefied RDF are in the range of 6.65–11.20 MJ kg^{-1} and 9.54–18.28 MJ kg^{-1} respectively, suggesting that the torrefaction pretreatment leads to a significant improvement in the LHV of the product gas. The profile of specific energy requirement (SER) of the untreated and torrefied RDF (Eq. (10)) is demonstrated in Fig. 8a, where untreated RDF displays the highest value of SER, implying that much higher plasma energy consumption is needed for generating syngas from the plasma gasification as compared to that of the torrefied RDF. Fig. 8b shows the overall plasma gasification efficiency (PGE) of the untreated and torrefied RDF as a function of S/F ratio, which is calculated by Eq. (7). It is clear that there exists an optimal value of PGE after undergoing torrefaction pretreatment. The optimal values of PGE of TR200-15, TR200-30, TR200-60, TR250-15, TR250-30, TR250-60, TR300-15, TR300-30, TR300-60 are 78.14%, 84.38%, 83.45%, 72.02%, 79.83%, 79.11%, 72.72%, 68.66%, and 66.68%, which occur at S/F = 0.08, 0.18, 0.18, 0.02, 0.18, 0.27, 0.26, 0.30, and 0.32, respectively. Notably, the maximum value of PGE for the untreated RDF is only 57.62%; therefore, the torrefaction pretreatment of RDF prior to the plasma gasification can considerably enhance the PGE. However, it should be noted that severe torrefaction conditions (i.e. 300 °C) lead to a lower value of PGE due to much higher energy demand from the torrefaction process (Table 3). The detailed performance of plasma gasification of various torrefaction conditions under their optimal S/F ratio is summarized in Table 6. To sum up, according to the obtained results shown above, it can be

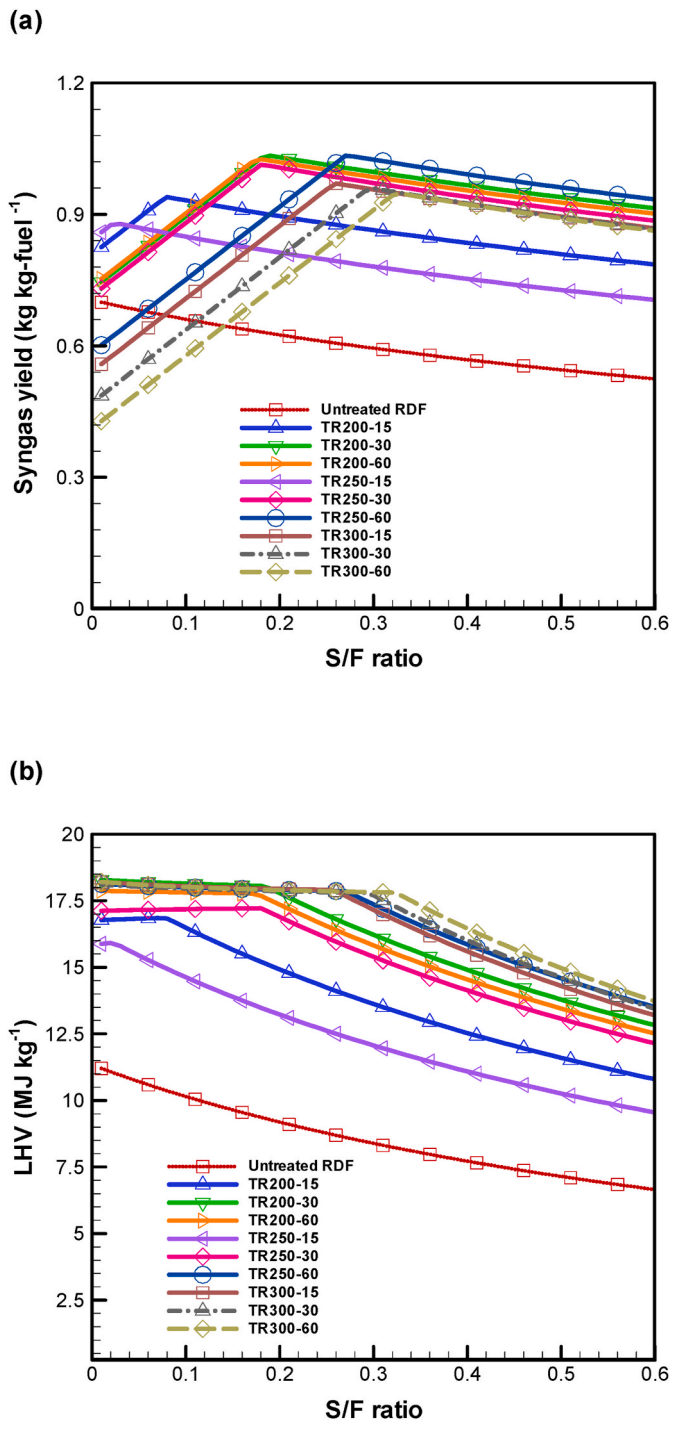

Fig. 7. Effect of S/F ratio on (a) syngas yield and (b) lower heating value of the product gas from the plasma gasifier.

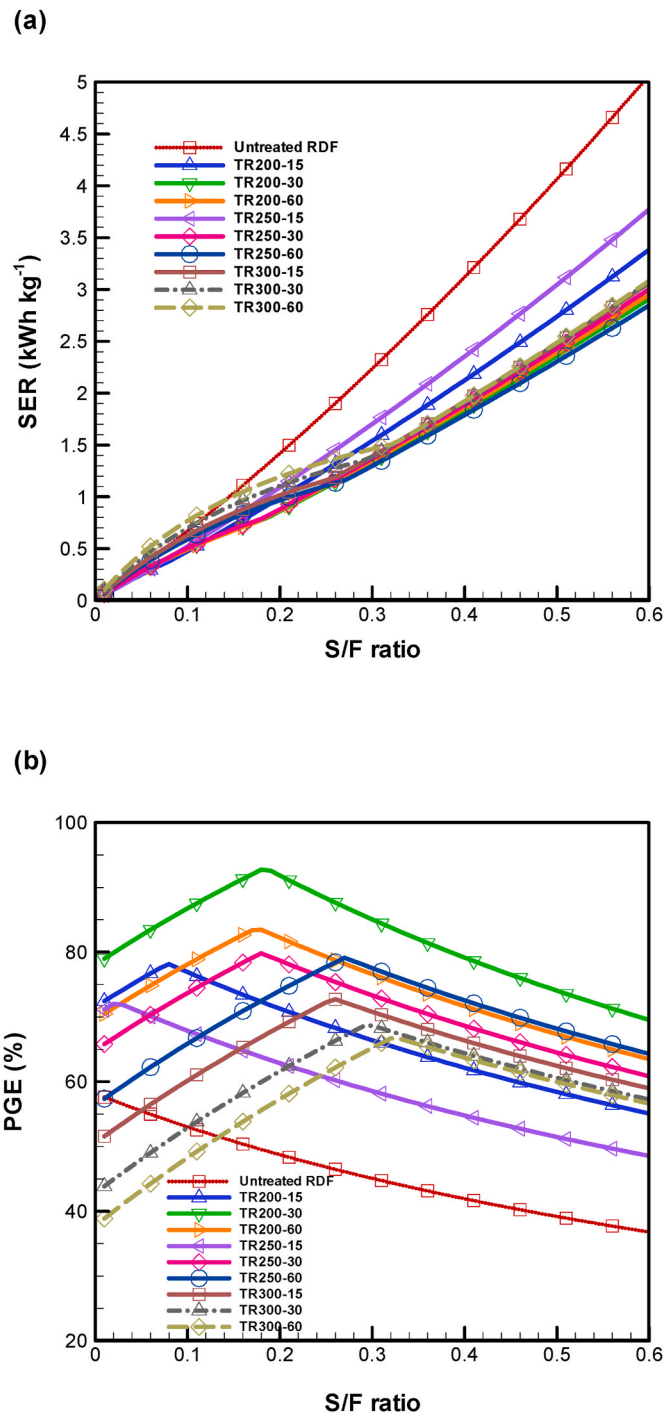

Fig. 8. Effect of S/F ratio on the performance of plasma gasifier: (a) specific energy requirement (SER) and (b) plasma gasification efficiency (PGE).

concluded that when a torrefaction pretreatment is employed prior to plasma gasification of RDF, it is able to improve the gasification performances in terms of syngas yield, SER, and PGE. Likewise, Recari et al. (2017) also reported that the gasification performance such as syngas quality, carbon conversion, tar levels, HCl concentration was enhanced when the solid recovered fuel (SRF) was torrefied.

3.2. Overall T-PG-SOFC-CHP system's performance

The effect of various torrefaction operating conditions on the energy and environmental performances of the T-PG-SOFC-CHP system including system electrical efficiency (SEE), combined heat and power efficiency (CHPE), energy return on investment (EROI) and specific CO_2 emissions (E_{CO_2}) are shown in Figs. 9 and 10. In order to compare the performance of T-PG-SOFC-CHP system at different torrefaction process conditions, the mass flowrate of RDF material is fixed at 50 kg h^{-1}, while a U_f of 0.85 and a RR of the anode off-gas of 0% are taken into account for the operation of SOFC. A comparison of SEE (Eq. (11)) and CHPE (Eq. (13)) between various cases is presented in Fig. 9a and b, where the values of SEE and CHPE are in the range of 21.56–45.24% and 31.14–55.39% respectively. Apparently, the values of SEE and CHPE decrease significantly when RDF is torrefied at 300 °C. The main reasons

Table 6
Performance of the plasma gasification at various torrefaction process conditions.

Torrefaction conditions (Temperature-Residence time)	Syngas yield (kg-fuel^{-1})	LHV (MJ kg^{-1})	SER for syngas production (kWh kg^{-1})	PGE (%)
TR200-15 (S/F = 0.08)	0.94	16.84	0.38	78.14
TR200-30 (S/F = 0.18)	1.03	18.06	0.78	84.38
TR200-60 (S/F = 0.18)	1.03	17.69	0.78	83.45
TR250-15 (S/F = 0.02)	0.88	15.91	0.10	72.02
TR250-30 (S/F = 0.18)	1.01	17.22	0.79	79.83
TR250-60 (S/F = 0.27)	1.03	17.86	1.16	79.11
TR300-15 (S/F = 0.26)	0.97	17.87	1.19	72.72
TR300-30 (S/F = 0.30)	0.96	17.71	1.39	68.66
TR300-60 (S/F = 0.32)	0.94	17.81	1.50	66.68

can be attributed to: (1) the higher S/F ratio needed in the plasma gasifier in order to maximize the SEE and CHPE (Table 6), leading to higher requirement of plasma energy; and (2) higher energy consumption required for the torrefaction process at 300 °C (Table 3). As a result, the values of SEE and CHPE obtained from RDF torrefaction at 300 °C are even much lower than that of the untreated RDF (without torrefaction), irrespective of the residence time. Fig. 10 shows a comparison of EROI (Eq. (14)) and E_{CO_2} (Eq. (16)) with respect to various torrefaction process conditions. It can be seen that the value of EROI for untreated RDF is around 4.22, which is the highest among all the cases. Despite the efficiency improvement in SEE and CHPE achieved via torrefaction, greater input energy associated with plasma gasification and torrefaction causes a lower value of EROI. TR250-15 has the highest value of EROI, which is about 3.79, among all torrefied RDF materials. In general, a minimum EROI of 3 is required in order to achieve a sustainable energy-producing system (Zhang and Colosi, 2013). Here, it has been shown that only untreated RDF (EROI = 4.22), TR200-15 (EROI = 3.10), and TR250-15 (EROI = 3.79) reach this criterion. Nevertheless, it should be noted that, in this work, the gaseous and liquid products released from the torrefaction process are not taken into account because of the insufficient information from the literature. In other words, if the energy recovery of gaseous and liquid products from torrefaction is further considered, the values of EROI could be enhanced. As far as the E_{CO_2} is concerned, Fig. 10b illustrates that it varies from around 0.83 to 2.75 kg kWh^{-1}. Among all the cases, TR250-15 has the lowest value (0.83 kg kWh^{-1}), followed by untreated RDF (0.89 kg kWh^{-1}) and TR200-15 (0.93 kg kWh^{-1}). The detailed results of the amount of total CO_2 emissions and total power output from the T-PG-SOFC-CHP system are given in Table 7, where it can be seen that although both direct and indirect CO_2 emissions of TR250-15 are slightly higher than those of untreated RDF, the net power output of TR250-15 is much higher than that of untreated RDF. This, in turn, results in relatively lower E_{CO_2} for TR250-15. In addition, the case of torrefaction at 300 °C exhibits relatively higher E_{CO_2}, especially for longer residence time. Again, this is because of a significant amount of indirect CO_2 emission related to energy consumption of torrefaction and plasma gasification.

To summarize, according to the observations in Figs. 9 and 10, severe torrefaction conditions (i.e. TR300-15, TR300-30, and TR300-60) give the worst energy and environmental performances and consequently they are not suitable to be utilized in the proposed T-PG-SOFC-CHP power plant. On the contrary, light and mild torrefaction conditions with a short residence time (i.e. TR200-15, TR200-30, and TR250-15) can not only effectively facilitate the energy efficiency of the T-PG-SOFC-CHP power plant, but also lessen the environmental impacts, especially when the energy recovery of gaseous and liquid products is further taken into account.

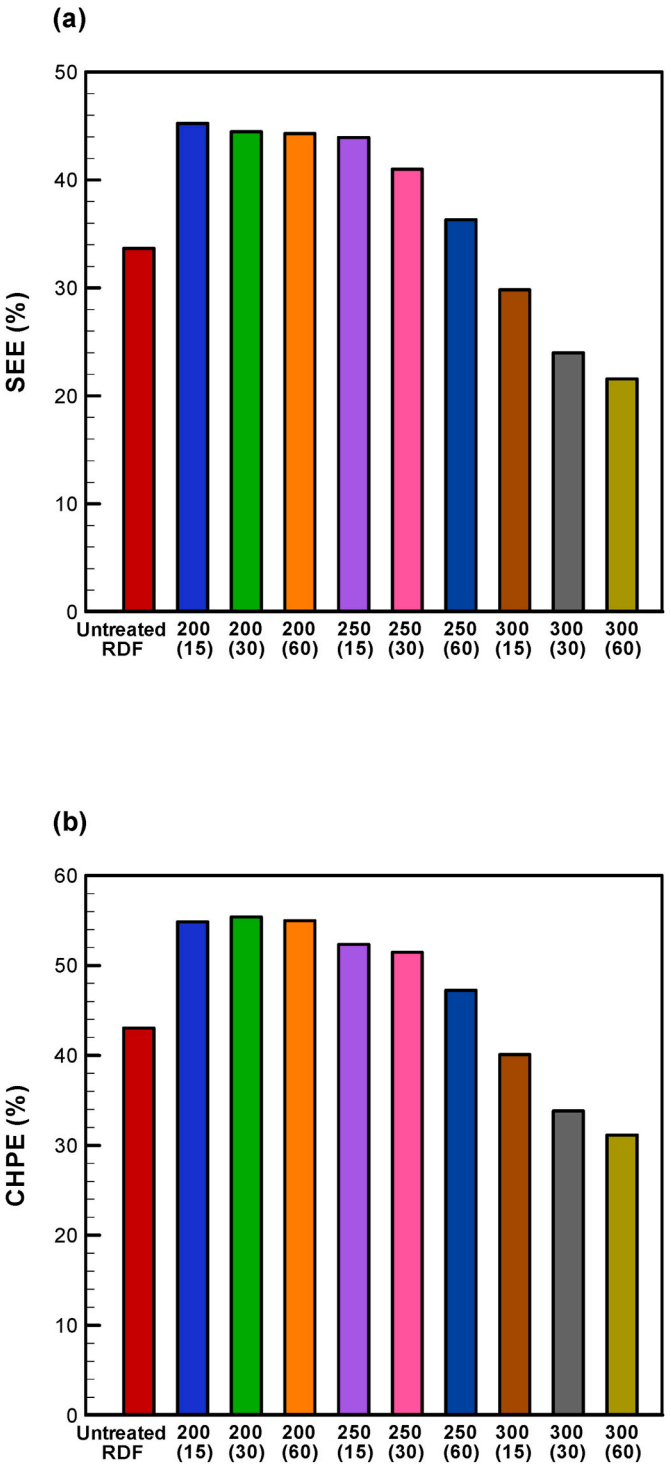

Fig. 9. Comparison of (a) system electrical efficiency (SEE) and (b) combined heat and power efficiency (CHPE) of the T-PG-SOFC-CHP power plant at various torrefaction conditions.

3.3. Sensitivity analysis

To determine the optimum operating conditions of the T-PG-SOFC-CHP system, the influences of U_f and RR of the anode-off gas on the energy and environmental performances are sequentially investigated. Based on the foregoing results from Figs. 9 and 10, the three torrefaction process conditions of TR200-15, TR200-30, and TR250-15 are appropriate to be used to in the proposed T-PG-SOFC-CHP system and hence

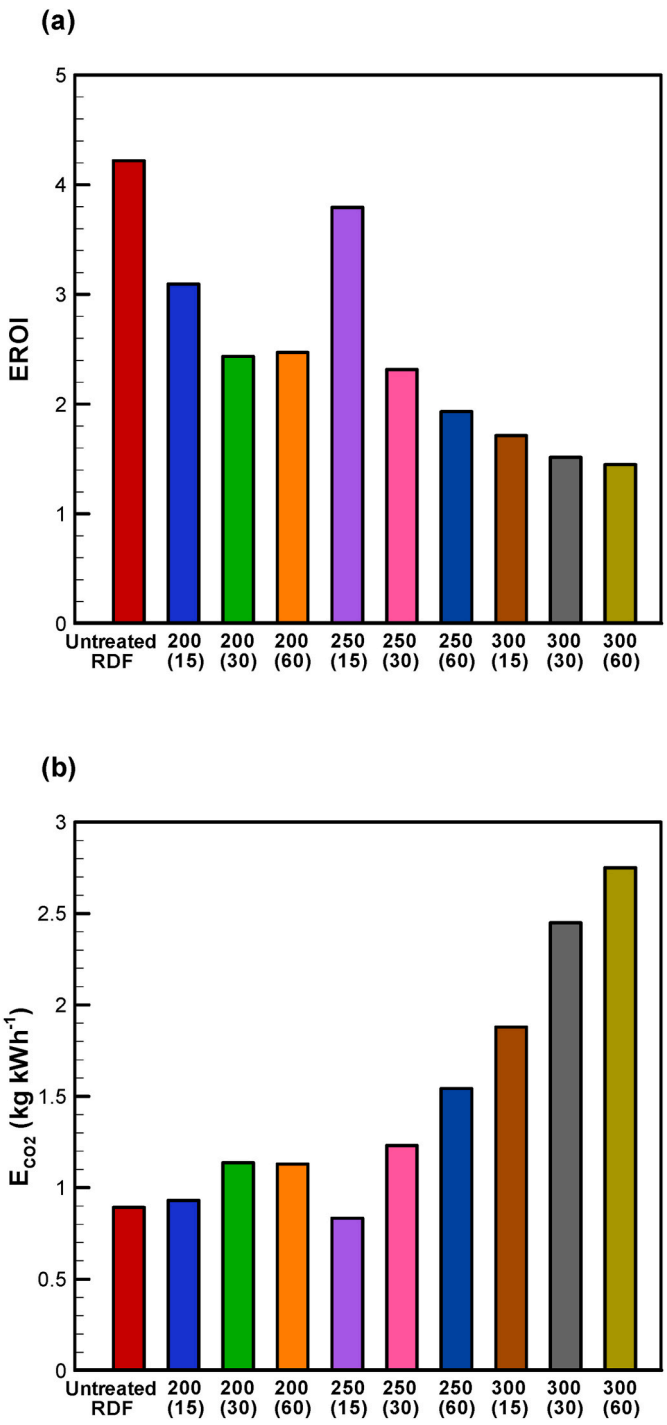

Fig. 10. Comparison of (a) energy return on investment (EROI) and (b) specific CO_2 emissions (E_{CO_2}) of the T-PG-SOFC-CHP power plant under various torrefaction process conditions.

these cases are considered to carry out various sensitivity analyses in this section.

3.3.1. Effect of fuel utilization factor

Fig. 11 shows the effect of U_f on the performance of SOFC and overall T-PG-SOFC-CHP system. Here, the S/F ratios of TR200-15, TR200-30, and TR250-15 are fixed at their optimal values (Table 6), while the inlet fuel flow rate and RR of the anode-off gas are kept constant at 50 kg h^{-1} and 0% respectively. It can be seen from Fig. 11a that when the U_f is raised from 0.65 to 0.90, the cell voltage decreases from 0.806 to 0.725 V, from 0.783 to 0.692 V, and from 0.822 to 0.749 V, whereas the current density increases from 1126.51 to 1559.78 A m^{-2}, 1314.94–1820.68 A m^{-2}, and 985.31–1364.27 A m^{-2}, corresponding to TR200-15, TR200-30, and TR250-15, respectively. According to Eq. (1), the increase of U_f leads to more hydrogen consumption by the SOFC, simultaneously resulting in an increase in current density (Eq. (1)). Therefore, a reduction of the cell voltage occurs as a result of increased polarization losses, especially at higher current density. Fig. 11b illustrates the impact of U_f on the overall T-PG-SOFC-CHP system efficiency in terms of SEE and CHPE. It is revealed that when U_f varies from 0.65 to 0.90, the values of SEE range from 40.64 to 46.30%, from 40.61 to 45.33%, and 39.62–44.75%, while those of CHPE change from 50.26 to 55.92%, from 51.53 to 56.25%, and from 48.05 to 53.18%, corresponding to TR200-15, TR200-30, and TR250-15, respectively. Due to the increase of electrical efficiency with U_f (Fig. 11b), Fig.. 11c and d indicate an increasing trend in EROI ranging from 2.87 to 3.14, 2.30 to 2.47, and 3.50 to 3.86 and a decreasing trend in the E_{CO_2} from 1.04 to 0.91 kg kWh^{-1}, 1.25 to 1.11 kg kWh^{-1}, and 0.91 to 0.81 kg kWh^{-1}, corresponding to TR200-15, TR200-30, and TR250-15 respectively.

3.3.2. Effect of recirculation ratio of the anode off-gas

It is well recognized from the literature that the carbon formation at the anode of SOFC is possible to occur when it is fed with the gasification syngas (Yi et al., 2005). One possible strategy to reduce the risk of carbon deposition in SOFCs is to increase the steam concentration in the inlet stream at the anode by recycling the anode-off gas (Colpan et al., 2007). The influence of RR of the anode off-gas, which is defined by Eq. (5), on the risk of carbon deposition is analyzed by using a C–H–O ternary diagram. As shown in Fig. 12, based on the thermodynamic equilibrium calculations obtained from Factsage software, the carbon boundary lines are plotted under three temperatures of 700 °C, 800 °C and 900 °C at 1 atm. The points shown in the C–H–O ternary diagram represents the inlet gas composition of the anode for the three cases obtained by varying the RRs from 0 to 40%. It is demonstrated that when the SOFCs is operated without recirculation of the anode-off gas (i.e. RR = 0%), the points for each case (i.e. TR200-15, TR200-30, and TR250-15) are nearly located at the carbon boundary line at the operating temperature of SOFC (i.e. 900 °C), indicating that the carbon deposition on the anode is likely to take place. However, with an increase in the RR, the points can be moved away from the carbon boundary line of 900 °C, no matter what cases are examined. This is mainly because a higher RR results in an increase in the steam concentration in the anode feed stream, which in turn promotes the mole fraction of oxygen. Accordingly, to ensure a safe operation for the SOFC and reformer in the operating temperature range between 700 and 900 °C, the RR of at least 30% for each case is recommended to be operated, since all the points lie in the carbon deposition-free region.

The influence of the RR on the performances of SOFC and overall T-PG-SOFC-CHP system with respect to each case is displayed in Fig. 13, where the inlet fuel flow rate and U_f are fixed at 50 kg h^{-1} and 0.85 respectively. Increasing the RR has a negative impact on the cell voltage (Fig. 13a), SEE and CHPE (Fig. 13b), as a result of the decreased SOFC power output caused by the increased steam partial pressure in the anode inlet gas. The observed results are in line with the simulated results from the works of Doherty et al. (2010) and Colpan et al. (2007), where they investigated the interaction between the anode recycle loop and the performance of SOFC fueled by gasification syngas. By virtue of the dropped SOFC power output, as shown in Fig. 13c and d, the values of EROI decrease while those of the E_{CO_2} increase with increasing RR.

3.4. Oxy-fuel combustion-based T-PG-SOFC-CHP power plant

From the aforementioned results, the proposed T-PG-SOFC-CHP power plant (System I) is able to offer high energy conversion efficiency, but CO_2 produced from the system is still directly emitted to the environment. To achieve a zero direct CO_2 emission power generation

Table 7
Performance of the T-PG-SOFC-CHP system at various torrefaction process conditions.

Torrefaction conditions (Temperature-Residence time)	TR200-15	TR200-30	TR200-60	TR250-15	TR250-30	TR250-60	TR300-15	TR300-30	TR300-60
Energy input breakdown (kW)									
Feedstock[a]	247.22	247.22	247.22	247.22	247.22	247.22	247.22	247.22	247.22
Torrefaction	25.14	24.58	22.64	25.28	25.69	24.58	34.58	37.22	36.81
Plasma gasification	17.74	39.90	39.90	4.43	39.90	59.86	57.64	66.51	70.94
Auxiliary power[b]	10.51	12.02	11.87	9.16	11.42	12.01	11.32	11.05	10.84
Energy output breakdown (kW)									
SOFC (AC)	99.64	111.46	109.95	89.81	107.11	111.19	106.54	104.58	103.22
HRSG	65.59	75.00	74.00	57.66	71.24	75.09	70.75	69.52	68.67
CO_2 emissions breakdown (kg h^{-1})									
CO_2 direct emissions	69.10	74.89	75.00	65.02	74.27	75.41	70.74	70.16	68.95
CO_2 indirect emissions[c]	34.97	50.12	48.74	25.46	50.45	63.18	67.82	75.18	77.68

Note.
[a] It is calculated based on LHV.
[b] Energy consumption from compressors and pumps.
[c] The CO_2 emission factor of 0.655 kg CO_2 kWh^{-1} is used (Ramirez et al., 2019).

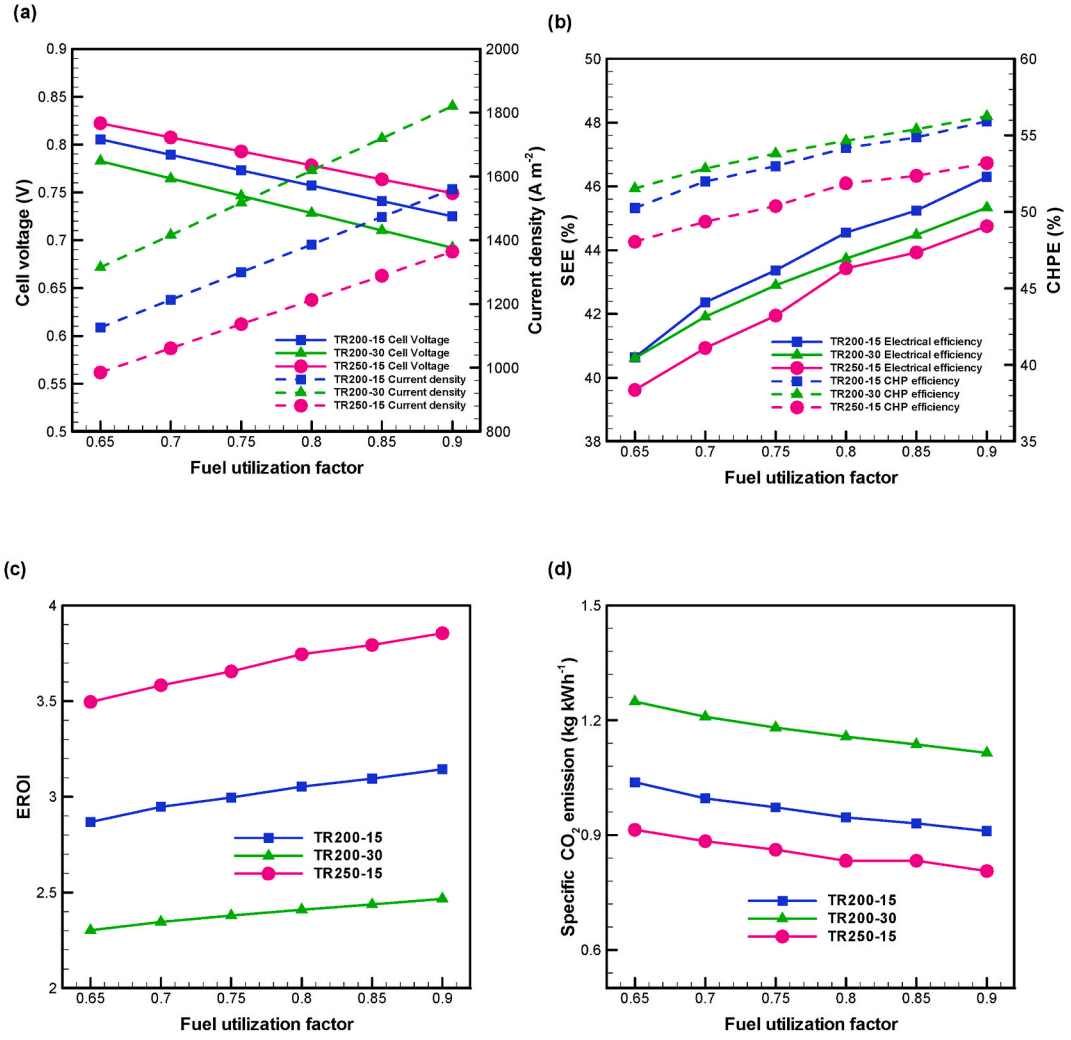

Fig. 11. Effect of fuel utilization factor (U_f) on (a) cell volage and current density, (b) SEE and CHPE, (c) EROI, and (d) specific CO_2 emissions.

system, an oxy-fuel combustion-based T-PG-SOFC-CHP power plant (System II) is designed (Fig. 4) and evaluated. The designed parameters of the oxy-fuel combustion system are listed in Table 1. A comparison of the performance indicators between System I and System II under the same process parameters (i.e. inlet fuel flow rate: 50 kg h^{-1}, U_f: 0.85, and RR: 30%) is given in Table 8. Furthermore, the main stream data of System I and System II for the case of TR200-15 is listed in Appendix (Table A1 and Table A2). It can be seen that the energy penalty related to the oxy-fuel based CO_2 capture technology is 5.40% for TR200-15, 6.77% for TR200-30, and 6.40% for TR250-15. Since System II contains an air separation unit and a CO_2 compression unit (Fig. 4), the additional energy requirement from these units in total is accounted for 21.05%, 16.15%, 27.19% of the auxiliary power, corresponding to TR200-15, TR200-30, and TR250-15 respectively. Additionally,

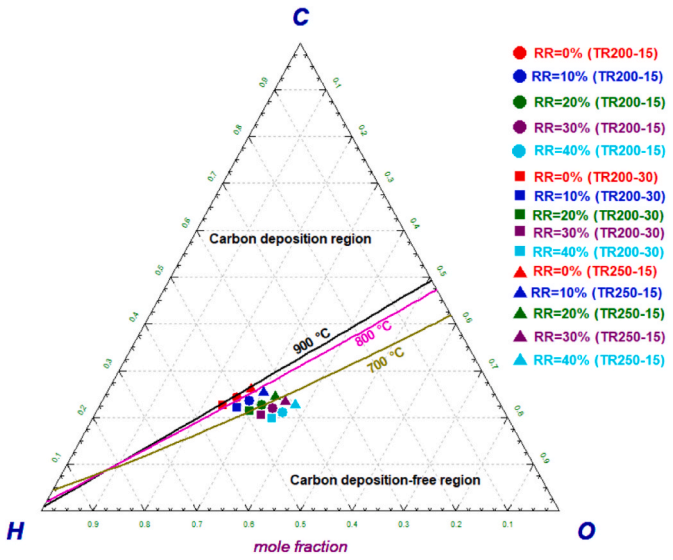

Fig. 12. Effect of recirculation ratio (RR) of the anode off-gas on carbon deposition behavior in the SOFC anode.

considering the environmental performance of the System II, when the oxy-fuel combustion technology is employed for the T-PG-SOFC-CHP power plant, although the values of EROI are reduced by 17.91%, 15.47%, and 23.06%, those of the E_{CO_2} are significantly decreased by 54.16%, 45.39%, and 58.91%, corresponding to TR200-15, TR200-30, and TR250-15, respectively. Obviously, the direct CO_2 emissions from the T-PG-SOFC-CHP power plant can be completely captured by using System II. However, to further reduce the indirect CO_2 emissions due to the major auxiliary power from torrefaction and plasma gasification, various renewable energy systems such as solar and wind energies (carbon-free electricity generation) could be integrated with the T-PG-SOFC-CHP power plant for intensifying WTE conversion technologies in the future.

4. Conclusions and future work

Aspen Plus modeling of an integrated torrefaction (T)-plasma gasification (PG)-solid oxide fuel cell (SOFC)-combined heat and power (CHP) power plant with and without CO_2 capture for the applications of WTE conversion process is successfully developed and analyzed in this work. The effect of untreated RDF (without torrefaction) and nine various torrefaction process conditions (i.e. TR200-15, TR200-30, TR200-60, TR250-15, TR250-30, TR250-60, TR300-15, TR300-30, and TR300-60) on the energy and environmental performances of the T-PG-SOFC-CHP power plant is evaluated and compared with each other. Based on the simulation results, the following major findings and

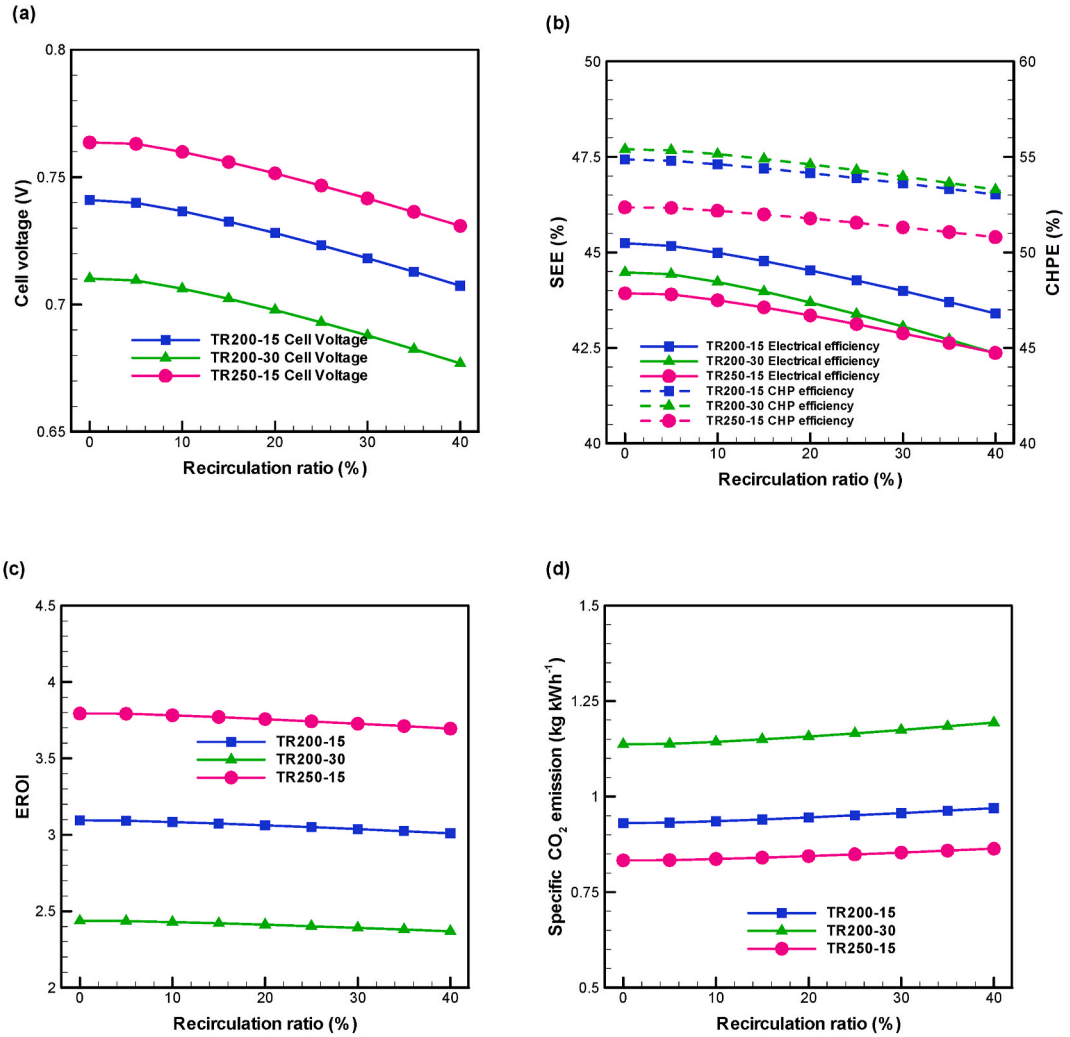

Fig. 13. Effect of recirculation ratio (RR) of the anode off-gas on (a) cell volage and current density, (b) SEE and CHPE, (c) EROI, and (d) specific CO_2 emissions.

Table 8
Performance of the oxy-fuel combustion-based T-PG-SOFC-CHP system with CO_2 capture (System II) (inlet fuel flow rate = 50 kg h^{-1}, U_f = 0.85, RR = 30%).

Configuration	System I			System II		
Torrefaction conditions (Temperature-Residence time)	TR200-15	TR200-30	TR250-15	TR200-15	TR200-30	TR250-15
Energy input breakdown (kW)						
Feedstock[a]	247.22	247.22	247.22	247.22	247.22	247.22
Torrefaction	25.14	24.58	25.28	25.14	24.58	25.28
Plasma gasification	17.74	39.90	4.43	17.74	39.90	4.43
Auxiliary power[b]	10.51	12.02	9.16	18.92	20.89	16.73
ASU[c]	–	–	–	2.11	2.46	1.84
Energy output breakdown (kW)						
SOFC (AC)	96.56	107.96	87.22	96.56	107.96	87.22
HRSG	65.58	75.00	57.66	62.75	69.59	51.25
CO_2 direct emissions	69.10	74.89	65.02	0	0	0
CO_2 indirect emissions[d]	34.97	50.12	25.46	41.86	57.53	31.63
System performance indicators						
SEE (%)	43.99	43.06	42.88	38.59	36.29	36.48
CHPE (%)	53.62	53.97	51.31	48.22	47.20	44.91
EROI (–)	3.04	2.39	3.73	2.49	2.02	2.87
E_{CO_2} (kg kWh^{-1})	0.96	1.17	0.85	0.44	0.64	0.35

Note.
[a] It is calculated based on LHV.
[b] Energy consumption for compressors and pumps.
[c] The specific energy consumption of 0.269 kWh kg^{-1} is used (Esfilar et al., 2018).
[d] The CO_2 emission factor of 0.655 kg CO_2 kWh^{-1} is used (Ramirez et al., 2019).

contributions from this study can be drawn:

(1) Integrating torrefaction of RDF with plasma gasification is a promising approach to significantly enhance the syngas yield and PGE. To achieve the maximum values of PGE, the optimal S/F ratios of TR200-15, TR200-30, and TR250-15 are 0.08, 0.18, and 0.02, respectively, at which those values are 78.14%, 84.38%, and 72.02%, respectively.
(2) Under the optimal S/F ratios, the torrefaction temperatures of 200 and 250 °C provide better energy performance in terms of SEE and CHPE, whereas they show negative impacts on environmental performances in terms of EROI and E_{CO_2}, with the exception of TR250-15, which even gives lower E_{CO_2} as compared to the untreated RDF. Basically, TR200-15, TR200-30, and TR250-15 are suggested to be used in the T-PG-SOFC-CHP power plant, whereas torrefaction of RDF at 300 °C is not feasible to the proposed system.
(3) To avoid the risk of carbon deposition on the SOFC anode, the recommend RR of the anode-off gas is 30%, at which the values of CHPE are 53.62%, 53.97%, and 51.31%, the values of EROI are 3.04, 2.39, and 3.73, and the values of E_{CO_2} are 0.96, 1.17, and 0.85 kg kWh^{-1}, corresponding to TR200-15, TR200-30, and TR250-15, respectively.
(4) A T-PG-SOFC-CHP power plant with zero direct CO_2 emissions is achievable by introducing the oxy-fuel combustion technology to the SOFC system. However, additional energy penalty of 5.40–6.77% is accompanied with such a new system. To reduce the indirect CO_2 emissions and increase the EROI, the various renewable energy technologies such as solar and wind should be integrated with the proposed WTE power plant.

The above optimal operating conditions of the T-PG-SOFC-CHP system are obtained based on a preliminarily thermodynamic assessment. Further numerical and dynamic simulation models are still required to be developed by considering both geometry and kinetic parameters. Therefore, more experimental works are needed to be carried out to find the detailed kinetic data for raw and torrefied RDF as feedstock for the plasma gasification. Also, the techno-economic analysis (TEA) of such a new WTE power plant should be explored for future research.

CRediT authorship contribution statement

Po-Chih Kuo: Conceptualization, Writing – review & editing. **Biju Illathukandy:** Conceptualization, Validation, Writing – review & editing. **Chi-Hsiu Kung:** Conceptualization. **Jo-Shu Chang:** Conceptualization, Writing – review & editing. **Wei Wu:** Conceptualization, Resources, Writing – review & editing.

Declaration of competing interest

The authors declare that they have no known competing financial interests or personal relationships that could have appeared to influence the work reported in this paper.

Acknowledgments

The authors would like to thank the Ministry of Science and Technology, Taiwan for the financial support of this research under the grant MOST 108-2917-I-564-039.

Appendix A. Supplementary data

Supplementary data to this article can be found online at https://doi.org/10.1016/j.jclepro.2021.128156.

References

Al-asadi, M., Miskolczi, N., Eller, Z., 2020. Pyrolysis-gasification of wastes plastics for syngas production using metal modified zeolite catalysts under different ratio of nitrogen/oxygen. J. Clean. Prod. 271, 122186.
Boesch, M.E., Vadenbo, C., Saner, D., Huter, C., Hellweg, S., 2014. An LCA model for waste incineration enhanced with new technologies for metal recovery and application to the case of Switzerland. Waste Manag. 34, 378–389.
Colpan, C.O., Dincer, I., Hamdullahpur, F., 2007. Thermodynamic modeling of direct internal reforming solid oxide fuel cells operating with syngas. Int. J. Hydrogen Energy 32, 787–795.
Doherty, W., Reynolds, A., Kennedy, D., 2010. Computer simulation of a biomass gasification-solid oxide fuel cell power system using Aspen Plus. Energy 35, 4545–4555.
Edo, M., Skoglund, N., Gao, Q., Persson, P.E., Jansson, S., 2017. Fate of metals and emissions of organic pollutants from torrefaction of waste wood, MSW, and RDF. Waste Manag. 68, 646–652.
Esfilar, R., Mehrpooya, M., Ali Moosavian, S.M., 2018. Thermodynamic assessment of an integrated biomass and coal cogasification, cryogenic air separation unit with power generation cycles based on LNG vaporization. Energy Convers. Manag. 157, 438–451.
Iroba, K.L., Baik, O.D., Tabil, L.G., 2017. Torrefaction of biomass from municipal solid waste fractions II: grindability characteristics, higher heating value, pelletability and moisture adsorption. Biomass Bioenergy 106, 8–20.
Janajreh, I., Raza, S.S., Valmundsson, A.S., 2013. Plasma gasification process: modeling, simulation and comparison with conventional air gasification. Energy Convers. Manag. 65, 801–809.
Kaza, S., Yao, L.C., Bhada-Tata, P., van Woerden, F., 2018. What a Waste 2.0: A Global Snapshot of Solid Waste Management to 2050. Washington, DC.
Kuo, P.C., Wu, W., 2016a. Design and thermodynamic analysis of a hybrid power plant using torrefied biomass and coal blends. Energy Convers. Manag. 111, 15–26.
Kuo, P.C., Wu, W., 2016b. Thermodynamic analysis of a combined heat and power system with CO_2 utilization based on co-gasification of biomass and coal. Chem. Eng. Sci. 142, 201–214.
Kuo, P.C., Wu, W., Chen, W.H., 2014. Gasification performances of raw and torrefied biomass in a downdraft fixed bed gasifier using thermodynamic analysis. Fuel 117, 1231–1241.
Liu, M., Woudstra, T., Promes, E.J.O., Restrepo, S.Y.G., Aravind, P.V., 2014. System development and self-sustainability analysis for upgrading human waste to power. Energy 68, 377–384.

Ma, W., Chu, C., Wang, P., Guo, Z., Liu, B., Chen, G., 2020. Characterization of tar evolution during DC thermal plasma steam gasification from biomass and plastic mixtures: parametric optimization via response surface methodology. Energy Convers. Manag. 225, 113407.
Manfredi, S., Christensen, T.H., 2009. Environmental assessment of solid waste landfilling technologies by means of LCA-modeling. Waste Manag. 29, 32–43.
Martínez, I., Arias, B., Grasa, G.S., Abanades, J.C., 2018. CO_2 capture in existing power plants using second generation Ca-Looping systems firing biomass in the calciner. J. Clean. Prod. 187, 638–649.
Mazzoni, L., Janajreh, I., 2017. Plasma gasification of municipal solid waste with variable content of plastic solid waste for enhanced energy recovery. Int. J. Hydrogen Energy 42, 19446–19457.
Minutillo, M., Perna, A., Bona, D.D., 2009. Modelling and performance analysis of an integrated plasma gasification combined cycle (IPGCC) power plant. Energy Convers. Manag. 50, 2837–2842.
Ng, K.S., Yang, A., Yakovleva, N., 2019. Sustainable waste management through synergistic utilisation of commercial and domestic organic waste for efficient resource recovery and valorisation in the UK. J. Clean. Prod. 227, 248–262.
Nobre, C., Vilarinho, C., Alves, O., Mendes, B., Gonçalves, M., 2019. Upgrading of refuse derived fuel through torrefaction and carbonization: evaluation of RDF char fuel properties. Energy 181, 66–76.
Perna, A., Minutillo, M., Lavadera, A.L., Jannelli, E., 2018. Combining plasma gasification and solid oxide cell technologies in advanced power plants for waste to energy and electric energy storage applications. Waste Manag. 73, 424–438.
Putna, O., Janoostak, F., Pavlas, M., 2020. Greenhouse gas credits from integrated waste-to-energy plant. J. Clean. Prod. 270, 122408.
Rago, Y.P., Collard, F.X., Görgens, J.F., Surroop, D., Mohee, R., 2020. Torrefaction of biomass and plastic from municipal solid waste streams and their blends: evaluation of interactive effects. Fuel 277, 118089.
Ramirez, A.D., Rivela, B., Boero, A., Melendres, A.M., 2019. Lights and shadows of the environmental impacts of fossil-based electricity generation technologies: a contribution based on the Ecuadorian experience. Energy Pol. 125, 467–477.
Recalde, M., Woudstra, T., Aravind, P.V., 2018. Renewed sanitation technology: a highly efficient faecal-sludge gasification–solid oxide fuel cell power plant. Appl. Energy 222, 515–529.
Recari, J., Berrueco, C., Puy, N., Alier, S., Bartrolí, J., Farriol, X., 2017. Torrefaction of a solid recovered fuel (SRF) to improve the fuel properties for gasification processes. Appl. Energy 203, 177–188.
Rutberg, P.G., Kuznetsov, V.A., Serba, E.O., Popov, S.D., Surov, A.V., Nakonechny, G.V., Nikonov, A.V., 2013. Novel three-phase steam-air plasma torch for gasification of high-caloric waste. Appl. Energy 108, 505–514.
Saleem, F., Harris, J., Zhang, K., Harvey, A., 2020. Non-thermal plasma as a promising route for the removal of tar from the product gas of biomass gasification-A critical review. Chem. Eng. J. 382, 122761.
Sheng, L., Liu, X., Si, J., Xu, Y., Zhou, Z., Xu, M., 2014. Simulation and comparative exergy analyses of oxy-steam combustion and O_2/CO_2 recycled combustion pulverized-coal-fired power plants. Int. J. Greenh. Gas Con. 27, 267–278.
Spies, K.A., Rainbolt, J.E., Li, X.S., Braunberger, B., Li, L., King, D.L., Dagle, R.A., 2017. Warm cleanup of coal-derived syngas: multicontaminant removal process demonstration. Energy Fuels 31, 2448–2456.
Thattai, A.T., Oldenbroek, V., Schoenmakers, L., Woudstra, T., Aravind, P.V., 2017. Towards retrofitting integrated gasification combined cycle (IGCC) power plants with solid oxide fuel cells (SOFC) and CO_2 capture-A thermodynamic case study. Appl. Therm. Eng. 114, 170–185.
Xiang, Y., Cai, L., Guan, Y., Liu, W., Liang, Y., Han, Y., Cao, Y., 2018. Influence of H_2O phase state on system efficiency in O_2/H_2O combustion power plant. Int. J. Greenh. Gas Con. 78, 210–217.
Xiang, Y., Cai, L., Guan, Y., Liu, W., Cheng, Z., Liu, Z., 2020. Study on the effect of gasification agents on the integrated system of biomass gasification combined cycle and oxy-fuel combustion. Energy 206, 118131.
Yi, Y., Rao, A.D., Brouwer, J., Samuelsen, G.S., 2005. Fuel flexibility study of an integrated 25kW SOFC reformer system. J. Power Sources 144, 67–76.
Zhang, Y., Colosi, L.M., 2013. Practical ambiguities during calculation of energy ratios and their impacts on life cycle assessment calculations. Energy Pol. 57, 630–633.
Zhang, W., Croiset, E., Douglas, P.L., Fowler, M.W., Entchev, E., 2005. Simulation of a tubular solid oxide fuel cell stack using Aspen Plus unit operation models. Energy Convers. Manag. 46, 181–196.